Quercetin as a Bitter Taste Receptor Agonist with Anticancer Effects in Head and Neck Cancer Cells

Gavin Turner[1], Sarah M. Sywanycz[1], Brianna L. Hill[1], Robert D. Wardlow, II[1], Robert J. Lee[1,2], Ryan M. Carey[1]*

[1] Department of Otorhinolaryngology – Head and Neck Surgery, University of Pennsylvania Health System, Philadelphia, PA 19104, USA

[2] Department of Physiology, Perelman School of Medicine, Philadelphia, PA 19104, USA

* Correspondence: ryan.carey@pennmedicine.upenn.edu

Abstract

Background/Objectives: Quercetin is a bitter compound with demonstrated anticancer effects in preclinical models of head and neck squamous cell carcinoma (HNSCC). In taste transduction, bitter compounds activate bitter taste receptors (T2Rs), a group of G protein-coupled receptors with downstream signaling that includes cytosolic calcium (Ca^{2+}) release. T2Rs are expressed in HNSCC cells, where their activation induces apoptosis *in vitro*. Increased T2R expression in HNSCC also correlates with improved patient survival. The objective of this study was to investigate the role of quercetin as an anticancer T2R agonist in HNSCC cells *in vitro* and *ex vivo*. **Methods**: Quercetin-mediated Ca^{2+} responses were assessed using live cell Ca^{2+} imaging in the presence of the T2R14 antagonist LF1 and G-protein inhibitor YM-254980 (YM) in UM-SCC-47 and FaDu HNSCC cell lines. Cell viability was evaluated using crystal violet assays in cell lines and MTS assays in patient-derived tumor slices. Mitochondrial depolarization was measured with TMRE in the presence and absence of T2R pathway inhibitors. **Results**: Quercetin induced a Ca^{2+} response in HNSCC cells, which was significantly reduced by LF1 and YM. Quercetin also decreased cell viability *in vitro* and showed a potential decrease in viability in tumor slices but was not statistically significant. Finally, quercetin caused mitochondrial depolarization, which was reduced in the presence of LF1 but not by YM. **Conclusions**: In HNSCC cells, quercetin causes a Ca^{2+} response that is likely mediated by T2R14, decreases viability, and causes mitochondrial depolarization.

Keywords: quercetin, bitter taste receptors, T2R14, calcium response, anticancer, mitochondrial depolarization, head and neck squamous cell carcinoma

1. Introduction

Head and neck cancers of the upper aerodigestive tract had a combined global incidence of over 890,000 cases in 2022 with projections rising to 1.37 million cases by 2045 [1, 2]. Natural compounds are being studied as potential anticancer agents, with plant flavonoids showing promise in pre-clinical models [3, 4]. Among them, quercetin – a flavanol widely distributed in fruits, vegetables, and medicinal plants – has been extensively investigated [4-6].

Quercetin is a bitter compound [7]; bitter compounds bind to bitter taste receptors (T2Rs), a family of G protein-coupled receptors (GPCRs) with approximately 25 isoforms in humans [8-10]. Canonical T2R signaling involves decreases in cAMP, increases in IP_3, release of endoplasmic reticulum calcium (Ca^{2+}) stores, and opening of TRP channels, leading to taste cell depolarization [11-20]. Beyond taste transduction, T2Rs are expressed extra-orally and have various actions: modulating innate immunity in airway epithelial cells via nitrous oxide production and increased ciliary beating, effecting hormone signaling in the gut through GLP-1 secretion, and promoting bronchodilation in airway smooth muscles via large-conductance Ca^{2+}-activated K^+ channel activation [21-24]. Importantly, T2Rs are also expressed in solid tumors, including HNSCC, where their activation has been linked to proteosome inhibition, apoptosis, and possibly mitochondrial Ca^{2+} overload and depolarization [25-27]. Increased T2R expression in HNSCC tumors correlates with improved patient survival, supporting a potential role for T2Rs as therapeutic targets [25]. Notably, the T2R14 agonist lidocaine has demonstrated anticancer effects [28-30], leading to clinical trials evaluating its efficacy for solid tumors such as breast cancer [31] and HNSCC [32].

Quercetin was initially shown to activate T2R14 and cause intracellular Ca^{2+} responses [33]. Subsequent studies confirmed quercetin binding to multiple T2Rs in HEK 293T cells and other cell types, including human choroid plexus papilloma cells and enteroendocrine L cells [34-

36]. While these findings support quercetin's role as a bitter agonist, further exploration is warranted to clarify its functional effects, signaling mechanisms, and target cell types. In this study, we show that quercetin induces intracellular Ca^{2+} responses in HNSCC cell lines that are likely T2R-mediated. We build upon prior evidence of quercetin's anticancer activity, demonstrating its ability to decrease HNSCC cell viability *in vivo* while exploring its effects in *ex vivo* tumor slices. Finally, we explore mitochondrial dynamics to evaluate the relationship between T2R activation and mitochondrial depolarization.

2. Materials and Methods

2.1 Cell Lines and Cell Culture

Human HNSCC cell lines included UM-SCC-47 ([SCC47] MilliporeSigma, St. Louis, MO USA; RRID: CVCL 7759) and FaDu (ATCC, Manassas, VA, USA; RRID: CVCL 1218). SCC47 is an HPV-positive HNSCC cell line derived from a tongue tumor of a 53-year-old male [37, 38]. The FaDu cancer cell line was derived from an HPV-negative tumor of the hypopharynx in a 56-year-old male [39]. Cells were cultured in high glucose Dulbecco's Modified Eagle's Medium (DMEM; Corning, Glendale, AZ, USA) supplemented with 10% FBS (Genesee Scientific, El Cajon, CA, USA), 1% penicillin/streptomycin (Gibco, Gaithersburg, MD, USA), and 1% nonessential amino acids (Gibco) at 37°C with CO_2 5%.

2.2 *Ex vivo* Tumor slices

Tumor tissue was acquired from HNSCC patients undergoing oncologic surgeries after written informed consent and approval of the University of Pennsylvania Institutional Review Board (IRB #417200). Specimens were embedded in agarose and sectioned into 300 μM slices

using a vibratome (Precisionary Compresstome Vibratome VF-510-0Z; oscillations 6 and speed 3). Slices were cultured free-floating in high glucose DMEM supplemented with 10% FBS, 1% penicillin/streptomycin, and 1% nonessential amino acids at 37 °C with 5% CO_2.

2.3 Reagents

Quercetin (Caymen Chemical Company, Ann Arbor, MI USA) 200 mM stock solutions were prepared in DMSO, aliquoted, and stored at -20 °C. Stocks were diluted into room temperature Hank's Balanced Salt Solution (HBSS) for live cell imaging or into 5% CO_2-equilibrated high glucose DMEM (with 10% FBS, 1% penicillin/streptomycin, and 1% nonessential amino acids) warmed to 37°C for viability assays. A maximally saturated working solution of quercetin was obtained by dissolving quercetin in HBSS at ≤500 μM with vortexing and shaking, followed by centrifugation to remove any small precipitates.

The T2R14 antagonist LF1 (Enamine, Monmouth Jct., NJ USA; Cat. No. Z85879385) was prepared as a 500 mM stock in DMSO, stored at -20 °C, and diluted to 500 μM in HBSS for experiments [40]. The $G\alpha_{q/11}$ inhibitor YM-254980 ([YM] Caymen Chemical Company, Ann Arbor, MI USA) was prepared as a 10 mM stock in DMSO, stored at -20 °C, and diluted to 1 μM in HBSS for experiments.

2.4 Live Cell Imaging

Live cell imaging was performed using an Olympus IX-83 microscope (20x 0.75 NA PlanApo objective) with appropriate filters (Semrock, Rochester, NY), an Orca Flash 4.0 sCMOS camera (Hamamatsu, Tokyo, Japan), MetaMorph Microscopy Automation and Image Analysis Software version 7.10.1.161 (Molecular Devices, San Jose, CA USA), and XCite 120 LED Boost

101 (Excelitas Technologies, Pittsburgh, PA). HBSS was used for fluorophore loading, washes,
102 imaging buffer, and experimental/control conditions. HBSS contained LF1 or YM for experiments
103 involving antagonists/inhibitors. Separate wells per plate were treated as technical replicates.
104 Repeating experiments with different cell passages were treated as biologic replicates.
105

106 2.4.1 Intracellular Ca^{2+} Dynamics

107 Cells were plated on 8-well glass bottom chamber slides (Cellvis, Mountain View, CA
108 USA). The next day, cells were incubated in Calbryte 590 acetoxymethyl ester (AM) (AAT
109 Bioquest, Pleasanton, CA USA) in HBSS for 45-60 minutes in the dark at room temperature, then
110 washed and maintained in imaging buffer as described in section 2.4 Live Cell Imaging. TRITC
111 filters (554/23 nm_{ex}, 609/54 nm_{em}, 573 nm long-pass dichroic; Semrock LED-TRITC-A-OMF)
112 were used. Imaging was performed with a 20x (0.8 NA) objective with 150 ms exposure of and
113 25% LED intensity at 15 second intervals. Baseline recordings were obtained before treatments.
114

115 2.4.2 Detecting autofluorescence

116 Cells were plated on 8-well glass bottom chamber slides. The next day, cells were washed
117 with HBSS and maintained in HBSS for imaging. FITC (474/27 nm_{ex}, 525/45 nm_{em}, 495 nm long-
118 pass dichroic; Semrock LED-FITC-A-OMF) and TRITC filters (described above) were used.
119 Imaging was performed with a 20x (0.8 NA) lens, 25% LED intensity, and 150 ms exposure at 45
120 second intervals for 22.5 minutes. Baseline images were acquired prior to treatments.
121

122 2.4.3 Mitochondrial Membrane Potential

123 Cells were plated on 8-well glass bottom chamber slides. The next day, cells were
124 incubated in HBSS with or without antagonist/inhibitor for 45 minutes, followed by incubation
125 with tetramethylrhodamine ethyl ester (TMRE) and Hoechst Dye (Caymen Chemical Company,
126 Ann Arbor, MI USA) for 15 minutes in the dark at room temperature. Cells were washed and
127 maintained in imaging buffer as described in section 2.4 Live Cell Imaging. DAPI filters were
128 used to initially identify nuclei, and TRITC filters were used for imaging. Cells were imaged at
129 20x with 50 ms exposure and 25% LED intensity at 20 second intervals.

130

131 2.5 Viability Assays

132 Cell viability of cell lines was assessed using crystal violet. Cells were seeded onto 24-well
133 plastic-bottom plates (Fisher Scientific) at 15% confluency for 48-hour experiments and 30% for
134 24-hour experiments and incubated at 37 °C with CO_2 5%. The following day, media was aspirated
135 and replaced with quercetin-containing media or control media. After 24 or 48 hours, cells were
136 washed with PBS, stained with crystal violet (0.1% in deionized water with 10% acetic acid), air-
137 dried, dissolved in 30% acetic acid, and absorbance measured at 590 nm using a Tecan Spark 10M
138 (Mannedorf, Switzerland). Technical triplicates were performed per condition with at least three
139 biological replicates.

140 Cell viability of tumor slices was assessed using the 3-(4,5-dimethylthiazol-2-yl)-5-(3-
141 carboxymethoxyphenyl)-2-(4-sulfophenyl)-2H-tetrazolium (MTS) assay. Slices were transferred
142 to individual wells of a 96-well plate (Fisher Scientific) containing 100 µL of phenol-free, high
143 glucose DMEM (supplemented with 10% FBS, 1% nonessential amino acids, and 1%
144 penicillin/streptomycin) with or without 200 µM quercetin, followed by incubation for 24 hours.
145 For each patient, three slices per condition were used, with three wells per condition lacking slices

146 to serve as blanks for background subtraction. At 22 hours, CellTiter 96 Aqueous One solution
147 MTS Cell Viability dye (Promega, Madison, WI, USA) was added to each well. At 24 hours,
148 supernatant was transferred to a new plate and absorbance analyzed at 490 nm using a Tecan Spark
149 10M.
150
151 2.6 Statistical Analysis
152 All analyses were performed using GraphPad Prism version 10.3.1 (GraphPad Software,
153 Boston, Massachusetts). When comparing two variables, unpaired t test was performed. Welch's
154 correction was performed when F test showed that the standard deviations of groups being
155 compared were significantly different. When comparing multiple variables, ordinary one-way
156 ANOVA followed by Tukey's multiple comparisons test comparing the mean of each column to
157 the mean of every other column was performed. Brown-Forsythe and Welch ANOVA test was
158 performed when Brown-Forsythe Test showed that the standard deviations of groups being
159 compared were significantly different. This was followed by Dunnet's T3 multiple comparisons
160 test comparing the mean of each column to the mean of every other column. For comparing
161 viability of tumor slices, Wilcoxon matched-pairs signed rank test was used. Statistical
162 significance for all experiments was set at $P < 0.05$.
163
164 **3. Results**
165
166 *3.1. Quercetin Causes an Intracellular Ca^{2+} Response that is Likely T2R-mediated*
167 Live-cell imaging with Calbryte 590 AM was used to measure cytosolic Ca^{2+} dynamics in
168 response to quercetin in SCC47 and FaDu cells. Maximum normalized fluorescence signals (F/F_0)

169 were significantly greater in quercetin-treated conditions compared to control (HBSS vehicle only)
170 in both cell lines, with average traces illustrating differences in signals over time (**Figure 1**). These
171 findings indicate that quercetin induces an intracellular Ca^{2+} response in HNSCC cells. To
172 determine whether these Ca^{2+} responses were T2R-mediated, experiments were repeated in the
173 presence of T2R14 antagonist LF1 [26, 40]. Peak F/F_0 signals after quercetin exposure were
174 significantly reduced in LF1-treated cells compared to control in both cell lines (**Figure 1**),
175 suggesting that T2R14 contributes to these Ca^{2+} responses.

176 To further test if the Ca^{2+} response is GPCR-mediated, live-cell imaging was conducted in
177 the presence of YM, a $G\alpha_{q/11}$ inhibitor [41]. In SCC47 cells, maximum normalized fluorescence
178 signals (F/F_0) were significantly lower with YM treatment compared to control (**Figure 2**). A
179 similar effect was observed in FaDu cells, where endpoint fluorescence signals after approximately
180 11 minutes of stimulation were signficantly reduced in YM-treated cells relative to control (**Figure**
181 **S1**).

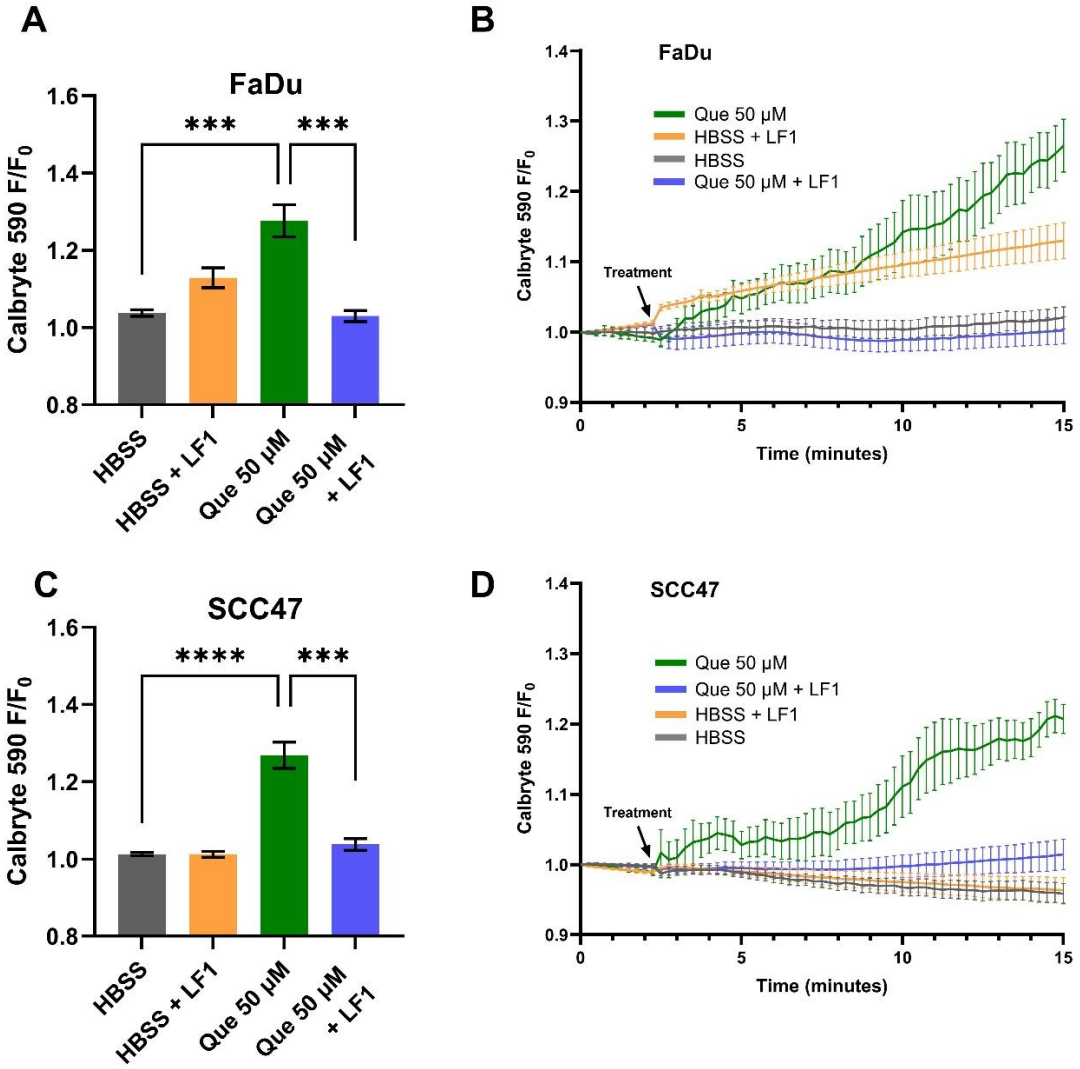

Figure 1. HNSCC cell line Ca^{2+} responses with quercetin in the presence and absence of T2R14 antagonist. Cells were incubated in Calbryte 590 AM with and without T2R14 antagonist LF1 prior to imaging. Quercetin with and without LF1 were added after baseline images were obtained; either HBSS or HBSS with LF1 served as the negative control. Cells were imaged at 20x using TRITC filters at 15 second intervals. Increased Calbryte 590 signal corresponds to increased intracellular Ca^{2+}. (**A**) Peak F/F_0 and (**B**) average traces with and without LF1 in FaDu cells. (**C**) Peak F/F_0 and (**D**) average traces with and without LF1 in SCC47 cells. Experiments were conducted with technical replicates with n = 4 and repeated with biologic replicates n = 3. The statistical method used was Brown-Forsythe and Welch ANOVA with Dunnet's T3 multiple comparisons test. Data points and error bars represent mean ± SEM. ***$P < 0.001$; ****$P < 0.0001$.

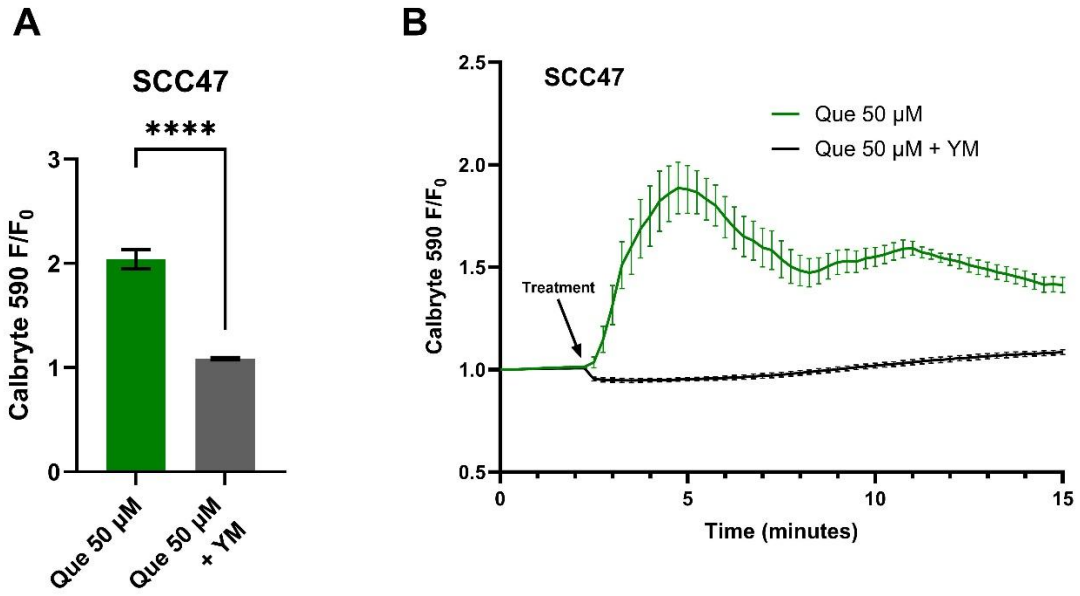

Figure 2. HNSCC cell line Ca^{2+} responses with quercetin in the presence and absence of $G\alpha_{q/11}$ inhibitor. SCC47 cells were incubated in Calbryte 590 AM with and without YM prior to imaging. Quercetin with and without YM were added after baseline images were obtained; HBSS with or without YM served as the negative controls respectively. Cells were imaged at 20x using TRITC filters at 15 second intervals. Increased Calbryte 590 signals correspond to increased intracellular Ca^{2+}. (**A**) Peak F/F_0 with and without YM and (**B**) average traces in SCC47 cells are shown. Experiments were conducted with technical replicates with n = 4 and repeated with biologic replicates n = 3. The statistical method used was Welch's t test. Data points and error bars represent mean ± SEM. ****$P < 0.0001$.

3.2. Intracellular Autofluorescence after Addition of Quercetin

To investigate the autofluorescent properties of quercetin in HNSCC cells, SCC47 and FaDu cells in the absence of fluorescent indicators were exposed to quercetin and imaged using FITC and TRITC filters. Upon addition of quercetin when using FITC filters, an immediate increase in fluorescent signals was observed and sustained over the approximate 23 minutes of imaging in both cell lines; no increases in fluorescence were observed when using TRITC filters (**Figure 3**). The increases in intracellular fluorescence when using FITC filters suggest at these

excitation/emission wavelengths that quercetin stimulation causes autofluorescence likely due to intracellular permeation and/or alteration of fluorescent properties of intracellular components in these cell lines [42]. Notably, the lack of autofluorescence at the TRITC wavelengths used for Calbryte 590 calcium imaging demonstrates that this autofluorescence would not affect our calcium data, but caution may be warranted when imaging other fluorophores with FITC wavelengths in experiments with quercetin.

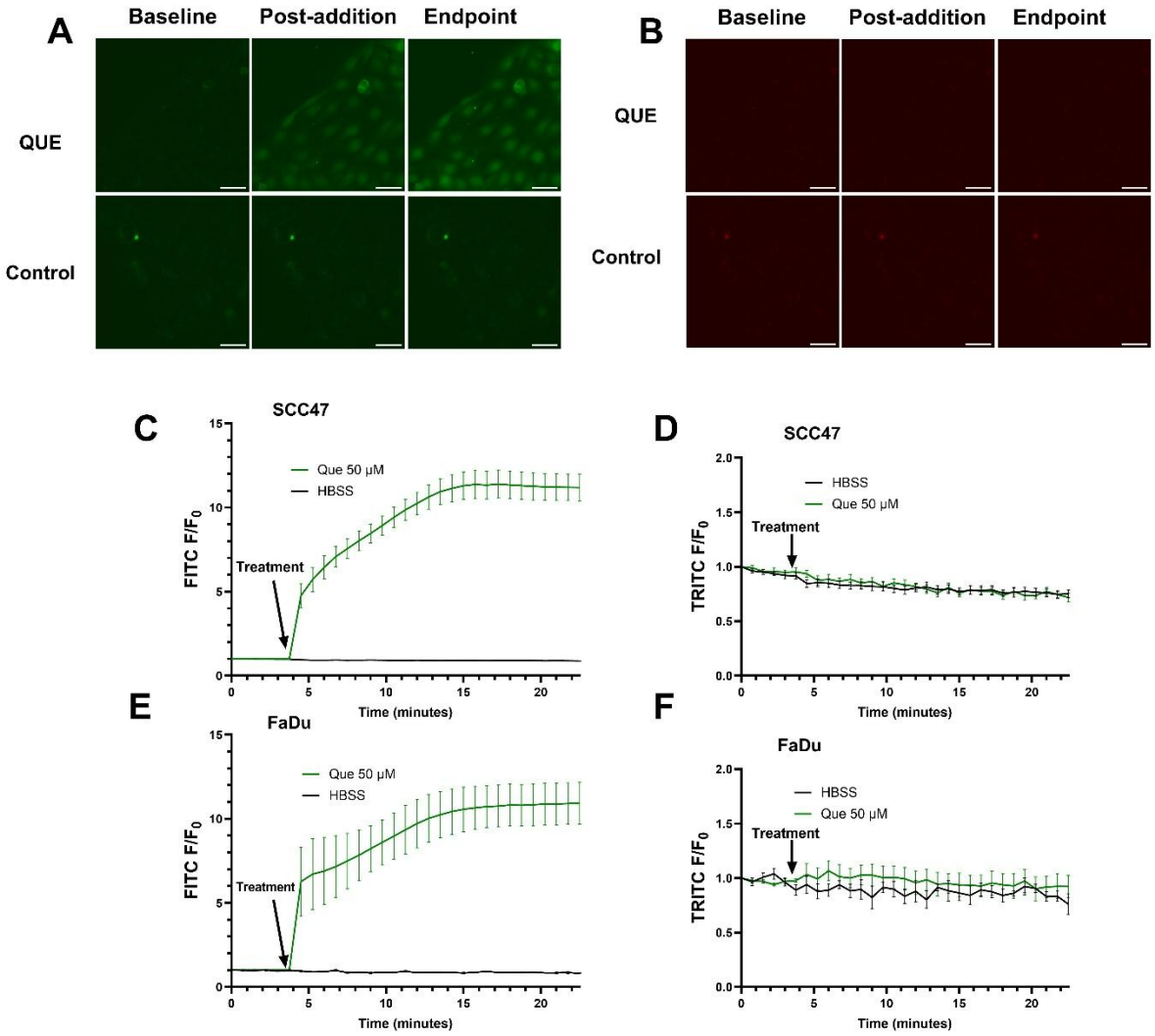

Figure 3. Autofluorescence detected in SCC47 and FaDu cells after addition of quercetin. Cells were washed and left in HBSS for imaging buffer, baseline images were acquired, and quercetin was added. FITC (474/27 nm_{ex}, 525/45

217 nm_{em}) and TRITC (554/23 nm_{ex}, 609/54 nm_{em}) filters were used to monitor autofluorescence signals. Cells were
218 imaged at 20x at 45 second intervals. Increased signal may correspond to quercetin autofluorescence in cells. (**A**)
219 Representative images in SCC47 cells using FITC and (**B**) TRITC filters. (**C**) Average traces in SCC47 using FITC
220 and (**D**) TRITC filters. (**E**) Average traces in FaDu cells using FITC and (**F**) TRITC filters. Scale bars in representative
221 images represent 50 μm. n = 4 technical replicates per condition with n = 3 biologic replicates in SCC47 and n = 1
222 biologic replicate in FaDu. Data points and error bars represent mean ± SEM.
223

224 *3.3. Quercetin Decreases Cell Viability*

225 To evaluate whether quercetin reduced cell viability in the studied HNSCC lines, crystal
226 violet assays were performed on SCC47 cells and FaDu cells after exposure to varying
227 concentrations of quercetin for 24 or 48 hours. Statistically significant decreases in viability were
228 observed beginning at 100 μM in both cell lines at both timepoints (**Figure 4**). For SCC47, the
229 IC_{50} values were 27.29 μM (95% CI: upper bound = 42.46 μM; lower bound could not be
230 determined) and 37.43 μM (95% CI: 23.48-56.71 μM) at 24 and 48 hours, respectively. For FaDu
231 cells, the IC_{50} values were 33.15 μM (95% CI: 24.27-40.84 μM) and 34.26 μM (95% CI: upper
232 bound = 45.50 μM; lower bound could not be determined) at 24 and 48 hours, respectively. These
233 findings suggest quercetin is cytotoxic to both HPV-positive and HPV-negative HNSCC cell lines
234 at micromolar concentrations.

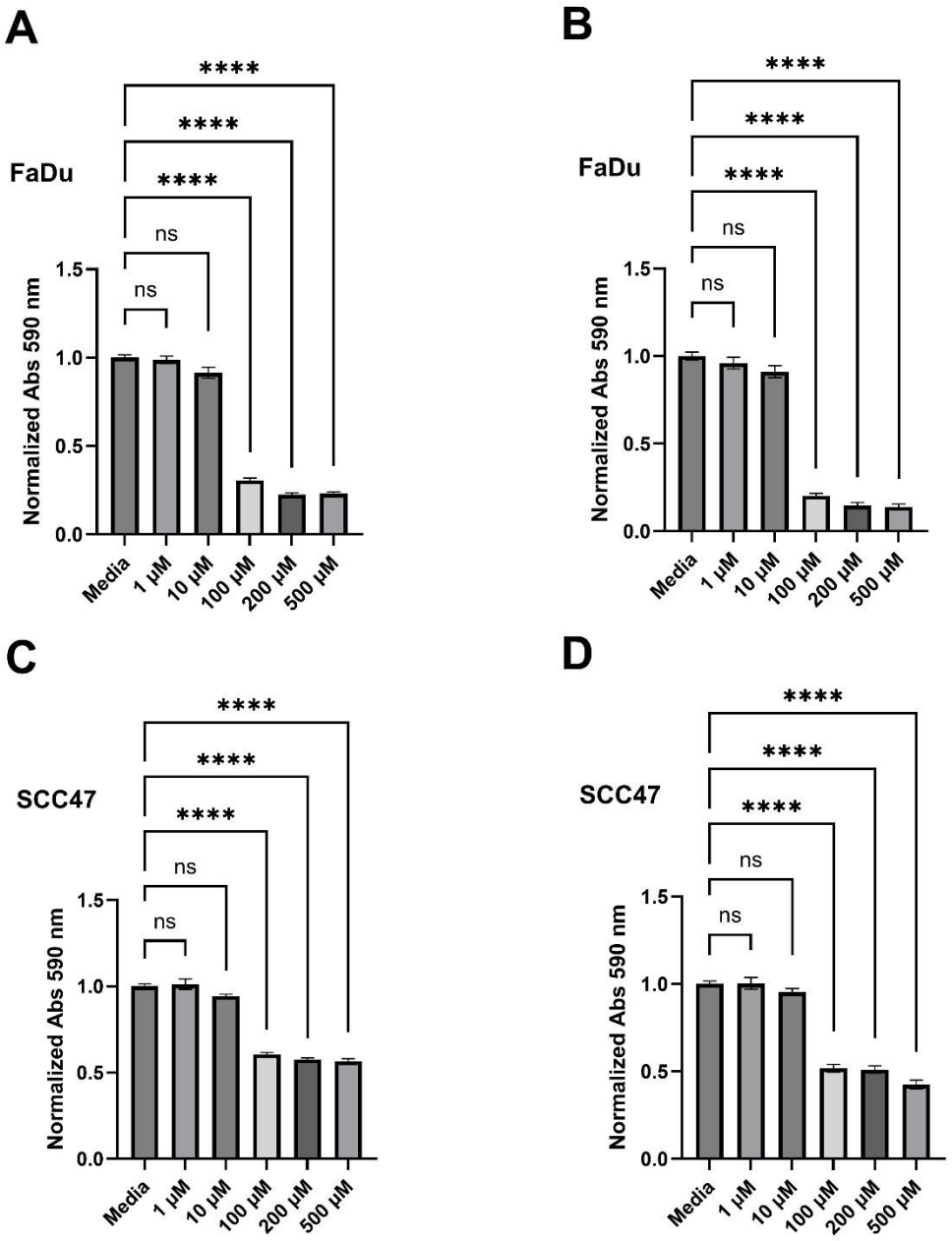

Figure 4. Quercetin decreases cell viability in HNSCC cell lines. Crystal violet assays were performed on SCC47 and FaDu cells treated with various concentrations of quercetin for either 24 or 48 hours. Media without quercetin was used as negative control in all experiments. (**A**) Cell viability after 24-hour and (**B**) 48-hour quercetin treatments in FaDu cells as assessed by crystal violet. (**C**) Cell viability after 24-hour and (**D**) 48-hour quercetin treatments in SCC47 cells assessed by crystal violet. Experiments were conducted with technical replicates with n = 3 and biologic replicates with n = at least 3. The statistical methods used were Brown-Forsythe and Welch ANOVA with Dunnet's

242 T3 multiple comparisons test (**A**) and ordinary one-way Anova with Tukey's multiple comparison test (**B-D**). Data
243 points and error bars represent mean ± SEM. ns, no statistical significance; ****P < 0.0001.
244
245 The effects of quercetin on viability were also assessed *ex vivo* using the MTS assay in
246 patient-derived tumor slices. Following 24-hour exposure to 200 μM quercetin or control, the
247 median of differences between control and treated samples was -0.31; however, Wilcoxon signed-
248 rank test indicated that this difference was not significant, W = -11.00, P = 0.19. A before-after
249 graph is shown in **Figure S2**. Given the limited sample size, additional studies with larger cohorts
250 and extended exposure times are warranted to more definitively assess quercetin's impact on tumor
251 slice viability. Demographic and tumor information is shown in **Table S1**.
252
253 *3.3 Quercetin Induces Mitochondrial Depolarization, Reduced by a T2R14 Antagonist*
254 Mitochondrial membrane potential was monitored using TMRE. In SCC47 cells, TMRE
255 minimum F/F_0 signals were significantly reduced following quercetin treatment compared to
256 control, with marked decreases observed within the first minute of quercetin exposure (**Figure 5**).
257 These results indicate that quercetin induces rapid mitochondrial depolarization.
258 In the presence of the T2R14 antagonist LF1, mitochondrial depolarization was still
259 observed, but minimum TMRE F/F_0 signals after 15 minutes were significantly greater compared
260 with quercetin alone (**Figure 5**). Similar findings were obtained in FaDu cells (**Figure S3**).
261 Interestingly, in the presence of $G\alpha_{q/11}$ inhibitor YM, quercetin did not cause significant differences
262 in minimum TMRE F/F_0 signals compared to control (**Figure S4**).

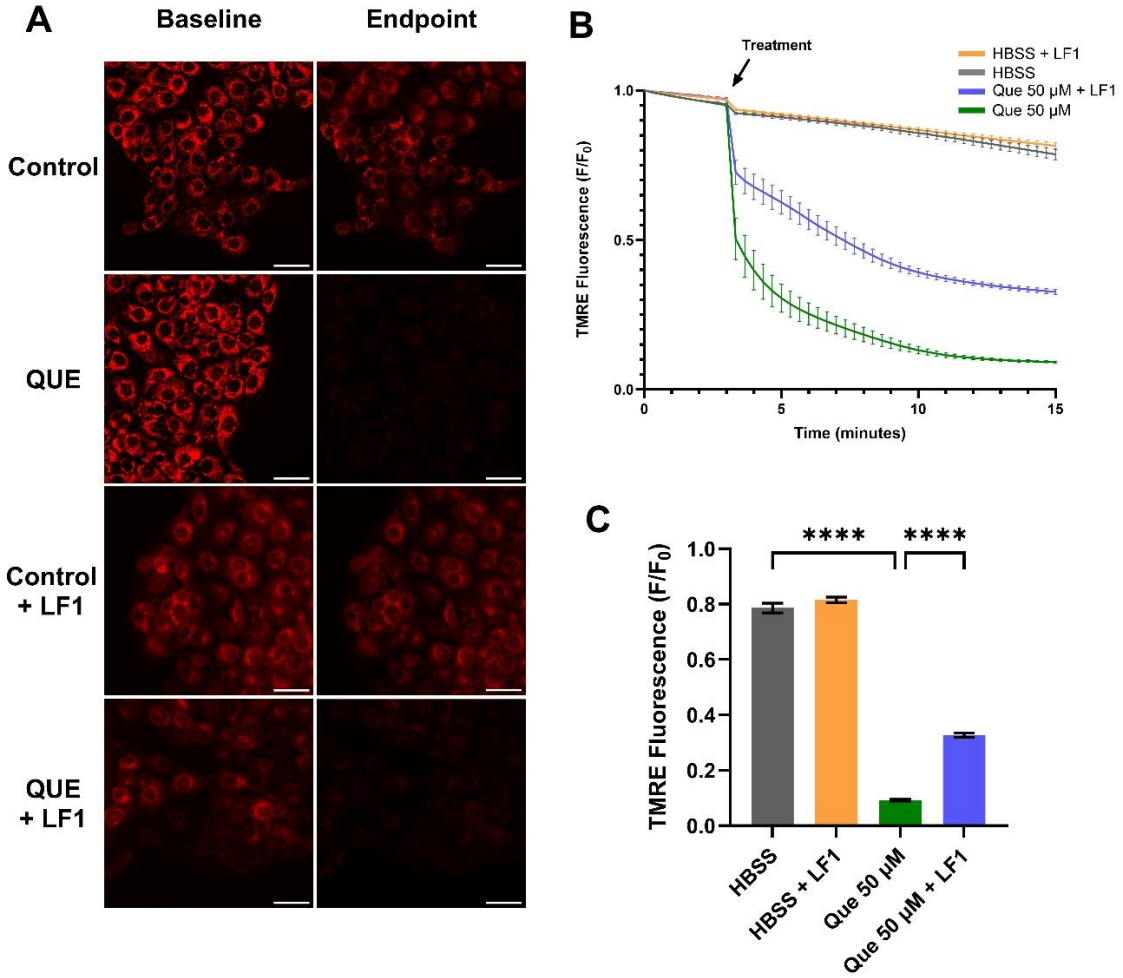

Figure 5. Mitochondrial depolarization in SCC47 cells exposed to quercetin with and without T2R antagonist LF1. Cells were incubated in TMRE and Hoechst dye with or without LF1 prior to imaging. Quercetin (with or without LF1) was added during imaging; HBSS or HBSS with LF1 served as negative controls. TMRE signal decreases when mitochondrial depolarization occurs. Cells were imaged at 20x using TRITC filters at 20 second intervals. (**A**) Representative images, (**B**) average traces, and (**C**) minimum TMRE F/F_0 with and without LF1 in SCC47 cells are shown. Scale bars represent 50 μm. Experiments were conducted with technical replicates with n = at least 3 and biologic replicates = 3. Statistical method used was Brown-Forsythe and Welch ANOVA with Dunnet's T3 multiple comparisons test. Data points and error bars represent mean ± SEM. ****$P < 0.0001$.

4. Discussion

274 In this study, we show that quercetin induces an intracellular Ca^{2+} response in HNSCC
275 cells, which is significantly reduced in the presence of $G\alpha_{q/11}$ inhibitor YM and T2R14 antagonist
276 LF1. These findings support the role of quercetin as a T2R agonist, with T2R14 playing a central
277 role in the observed Ca^{2+} responses. T2Rs interact with various G-proteins, with Ca^{2+} responses
278 mostly dependent on Gβγ-mediated PLCβ activity [19, 25]. YM, a $G\alpha_{q/11}$ inhibitor described as an
279 "allosteric glue" that stabilizes the G-protein heterotrimer [43], reduced fluorescence signals,
280 suggesting that quercetin-induced Ca^{2+} responses are likely mediated through $G\alpha_{q/11}$ and associated
281 Gβγ subunits. The reductions observed with LF1 further implicate T2R14 specifically, consistent
282 with reports of LF1 as a selective T2R14 antagonist [26, 40].

283 Our findings expand upon prior reports that quercetin activates T2Rs. While initially
284 identified as a T2R14 agonist, quercetin has since been shown to activate several additional
285 receptors (e.g., T2R4, T2R7, T2R10, T2R31, T2R39, T2R40, T2R43, T2R46) in HEK293T cells,
286 with the strongest Ca^{2+} response via T2R14 [33, 34]. In other cell types, such as human NCI-H716
287 intestinal L-cells and human choroid plexus papilloma cells, quercetin has been shown to enhance
288 GLP-1 secretion via T2R38 [35] and trigger T2R14-mediated Ca^{2+} responses confirmed by
289 knockdown [36]. Notably, in SCC47 and FaDu cells—which express multiple T2Rs [25, 26]—
290 T2R14 antagonism alone was sufficient to significantly reduce quercetin-induced Ca^{2+} responses,
291 suggesting that while quercetin may bind multiple receptors, its predominant effects in HNSCC
292 cells are mediated through T2R14.

293 We also demonstrated autofluorescence in SCC47 and FaDu cells after addition of
294 quercetin when using FITC filters, aligning with prior observations in HepG2 cells at similar
295 excitation/emission ranges [42]. These results suggest intracellular accumulation of quercetin.

296 Given that T2R14 has both extracellular and intracellular binding sites [44-46], these findings raise
297 the possibility that quercetin's effects may result from interactions at one or both sites.
298 Quercetin significantly decreased cell viability in SCC47 and FaDu cells, consistent with previous
299 reports of quercetin's cytotoxicity in various HNSCC lines [47]. In SCC47, absorbance values for
300 conditions reducing viability were typically 50–60% of control, while in FaDu cells, viability
301 reductions were greater at 20–30% of control. These differences between cell lines may reflect
302 inherent variation in adherence and growth characteristics between the two lines or different
303 susceptibility to quercetin.

304 *Ex vivo* studies using patient-derived tumor slices were more limited. Although the viability
305 in some cases were decreased after treatment with quercetin, the results overall were not
306 statistically significant with definitive conclusions potentially being limited by our sample size.
307 Importantly, tumor slice models preserve elements of the tumor microenvironment—including
308 immune cells and stromal cells [48]—which may influence therapeutic responses and the observed
309 effects on viability when using the MTS assay. Future studies with larger cohorts are needed to
310 determine whether quercetin decreases tumor slice viability and to evaluate potential effects on
311 normal tissue.

312 Quercetin's known ability to induce apoptosis may explain the reduced cell viability
313 observed [49-53]. Prior studies in HNSCC and other cancers suggest contributions from
314 mitochondrial depolarization and intrinsic apoptotic pathways [49, 51, 53-55]. Consistent with
315 this, we observed quercetin-induced mitochondrial depolarization by TMRE imaging. LF1
316 partially mitigated this effect, whereas YM did not alter depolarization, suggesting that quercetin's
317 effects on mitochondrial membrane potential may involve mechanisms in addition to $G\alpha_{q/11}$-
318 mediated T2R signaling. Potential alternative mechanisms for quercetin-induced apoptosis include

activation of mitochondrial large-conductance Ca^{2+}-regulated potassium channels or interactions with the mitochondrial permeability transition pore [56, 57]. These findings do not definitively link T2R signaling to mitochondrial-driven decreases in viability during quercetin stimulation, and they underscore the complexity of quercetin's mechanisms in HNSCC cells.

This study has limitations. Pharmacologic antagonists were used rather than T2R knockdown/knockout models, which would more definitively establish receptor specificity. Additional limitations include the small number of cell lines tested and small sample size for *ex vivo* tumor slices. Investigation in further cells lines, larger sample sizes for *ex vivo* models, and animal or patient-derived xenograft models are needed to better understand the potential T2R-mediated anti-cancer effects of quercetin in HNSCC tumors.

Overall, this work supports quercetin as a T2R agonist that induces intracellular Ca^{2+} responses in HNSCC cells, with T2R14 playing a key role. These findings contribute to the growing evidence for extra-oral T2Rs in cancer biology. Future studies using genetic knockdown or knockout approaches could more definitively define T2R14's contribution. *Ex vivo* tumor slice models will be particularly valuable for validating mechanistic findings and assessing translational potential, especially given species differences between human and rodent T2Rs [34]. Finally, because many plant flavonoids and polyphenols are bitter compounds [58] with anticancer [3, 4] and anti-inflammatory properties [59], broader investigation of flavonoid T2R agonism in extra-oral tissues is warranted [60]. Beyond HNSCC, such studies may reveal novel roles for T2R signaling in normal physiology, disease pathophysiology, and therapeutic targeting.

5. Conclusions

This study demonstrates that quercetin induces intracellular Ca^{2+} responses in HNSCC cell lines, which are significantly reduced by the $G\alpha_{q/11}$ inhibitor YM and the T2R14 antagonist LF1, supporting a key role for T2R14 in mediating these effects. Quercetin also decreases cell viability and promoted mitochondrial depolarization, adding to the evidence of its anticancer activity in HNSCC. Together, these findings identify quercetin as a functional T2R14 agonist in HNSCC cells and highlight the importance of extra-oral T2R signaling in tumor biology. While prior work has linked T2R activation to apoptosis, further studies are needed to clarify the mechanistic connection between quercetin-induced T2R signaling, mitochondrial dynamics, and cell death. These results suggest that targeting T2R14 signaling with quercetin or related compounds may represent a novel therapeutic strategy for HNSCC.

Supplementary Materials: Additional Supplemental Figures can be found online in the Supplementary Material Tab. Figure S1: Live cell Ca^{2+} imaging in FaDu cells stimulated with quercetin in the presence and absence of $G\alpha_{q/11}$ inhibitor; Figure S2: Effects of quercetin on cell viability of tumor slices; Table S1: Clinical data for HNSCC patients; Figure S3: Mitochondrial depolarization in FaDu cells exposed to quercetin with and without T2R Antagonist LF1; Figure S4: Mitochondrial depolarization assessed in SCC47 cells exposed to quercetin in the presence and absence of $G\alpha_{q/11}$ inhibitor.

Author Contributions: Conceptualization, Turner, G., Sywanycz, S., Hill, B., Wardlow, R., Lee, R., and Carey, R.; methodology, Turner, G., Sywanycz, S., Hill, B., Wardlow, R., Lee, R., and Carey, R.; formal analysis, Turner, G., Sywanycz, S., Hill, B., Wardlow, R., Lee, R., and Carey, R.; investigation, Turner, G., Sywanycz, S.; writing—original draft preparation, Turner, G.;

writing—review and editing, Turner, G., Sywanycz, S., Hill, B., Wardlow, R., Lee, R., and Carey, R.; visualization, Turner, G.; supervision, Lee, R., and Carey, R.; All authors have read and agreed to the published version of the manuscript.

Funding: This study was supported by a McCabe Foundation Fellowship Grant (RMC) and US National Institutes of Health grants R01AI167971 (RJL) and R01DE034474 (RMC).

Institutional Review Board Statement: The study was conducted in accordance with the Declaration of Helsinki, and approved by the Institutional Review Board of the University of Pennsylvania (protocol code 417200 approved 1/8/2025).

Informed Consent Statement: Informed consent was obtained from all subjects involved in the study.

Data Availability Statement: All data are contained within the manuscript, and other raw data are available upon request.

Acknowledgments: We would like to acknowledge M. Victoria for her technical expertise and assistance.

Conflicts of Interest: The authors declare no conflicts of interest.

Abbreviations

387 The following abbreviations are used in this manuscript:

Ca^{2+}	Calcium
DMEM	Dulbecco's Modified Eagle Medium
DMSO	Dimethyl sulfoxide
FBS	Fetal Bovine Serum
GPCR	G-protein coupled receptor
HBSS	Hank's Balanced Salt Solution
HNSCC	Head and neck squamous cell carcinoma
IP_3	Inositol triphosphate
MTS	3-(4,5-dimethylthiazol-2-yl)-5-(3-carboxymethoxyphenyl)-2-(4-sulfophenyl)-2H-tetrazolium
PLCβ	Phospholipase Cβ
T2R	Bitter taste receptor
TMRE	Tetramethylrhodamine ethyl ester
YM	YM-254980

388

389 **References**

390 1. Bray, F.; Laversanne, M.; Sung, H.; Ferlay, J.; Siegel, R. L.; Soerjomataram, I.; Jemal, A. Global
391 cancer statistics 2022: GLOBOCAN estimates of incidence and mortality worldwide for 36
392 cancers in 185 countries. *CA: A Cancer Journal for Clinicians* **2024**, *74* (3), 229-263. DOI:
393 10.3322/caac.21834.
394 2. Ferlay J, L. M., Ervik M, Lam F, Colombet M, Mery L, Piñeros M, Znaor A, Soerjomataram I,
395 Bray F. *Global Cancer Observatory: Cancer Tomorrow (version 1.1).* Lyon, France: International
396 Agency for Research on Cancer, 2024. https://gco.iarc.who.int/tomorrow (accessed 2025 July 13).

397 3. Mir, S. A.; Dar, A.; Hamid, L.; Nisar, N.; Malik, J. A.; Ali, T.; Bader, G. N. Flavonoids as
398 promising molecules in the cancer therapy: An insight. *Current Research in Pharmacology and*
399 *Drug Discovery* **2024**, *6*, 100167. DOI: 10.1016/j.crphar.2023.100167.
400 4. Rauf, A.; Imran, M.; Khan, I. A.; Ur-Rehman, M.; Gilani, S. A.; Mehmood, Z.; Mubarak, M. S.
401 Anticancer potential of quercetin: A comprehensive review. *Phytotherapy Research* **2018**, *32* (11),
402 2109-2130. DOI: 10.1002/ptr.6155.
403 5. Silva-Pinto, P. A.; De Pontes, J. T. C.; Aguilar-Morón, B.; Canales, C. S. C.; Pavan, F. R.;
404 Roque-Borda, C. A. Phytochemical insights into flavonoids in cancer: Mechanisms, therapeutic
405 potential, and the case of quercetin. *Heliyon* **2025**, *11* (4), e42682. DOI:
406 10.1016/j.heliyon.2025.e42682.
407 6. Sultana, B.; Anwar, F. Flavonols (kaempeferol, quercetin, myricetin) contents of selected fruits,
408 vegetables and medicinal plants. *Food Chemistry* **2008**, *108* (3), 879-884. DOI:
409 10.1016/j.foodchem.2007.11.053.
410 7. Huang, M.; Cong, L.; Ying, R.; Ahmad, M.; Hao, G.; Hayat, K.; Salamatullah, A. M.
411 Polysaccharide-coated quercetin-loaded nanoliposomes mitigate bitterness: A comparison of
412 carrageenan, pectin, and trehalose. *International Journal of Biological Macromolecules* **2024**, *259*,
413 129410. DOI: 10.1016/j.ijbiomac.2024.129410.
414 8. Meyerhof, W. Elucidation of mammalian bitter taste. Springer Berlin Heidelberg, 2005; pp 37-
415 72.
416 9. Behrens, M.; Foerster, S.; Staehler, F.; Raguse, J.-D.; Meyerhof, W. Gustatory Expression
417 Pattern of the Human TAS2R Bitter Receptor Gene Family Reveals a Heterogenous Population of
418 Bitter Responsive Taste Receptor Cells. *The Journal of Neuroscience* **2007**, *27* (46), 12630-12640.
419 DOI: 10.1523/jneurosci.1168-07.2007.
420 10. Hoon, M. A.; Adler, E.; Lindemeier, J.; Battey, J. F.; Ryba, N. J. P.; Zuker, C. S. Putative
421 Mammalian Taste Receptors. *Cell* **1999**, *96* (4), 541-551. DOI: 10.1016/s0092-8674(00)80658-3.
422 11. Akabas, M. H.; Dodd, J.; Al-Awqati, Q. A Bitter Substance Induces a Rise in Intracellular
423 Calcium in a Subpopulation of Rat Taste Cells. *Science* **1988**, *242* (4881), 1047-1050. DOI:
424 10.1126/science.3194756.
425 12. Huang, L.; Shanker, Y. G.; Dubauskaite, J.; Zheng, J. Z.; Yan, W.; Rosenzweig, S.; Spielman,
426 A. I.; Max, M.; Margolskee, R. F. Gγ13 colocalizes with gustducin in taste receptor cells and

427 mediates IP3 responses to bitter denatonium. *Nature Neuroscience* **1999**, *2* (12), 1055-1062. DOI:
428 10.1038/15981.
429 13. Wong, G. T.; Gannon, K. S.; Margolskee, R. F. Transduction of bitter and sweet taste by
430 gustducin. *Nature* **1996**, *381* (6585), 796-800. DOI: 10.1038/381796a0.
431 14. Hwang, P. M.; Verma, A.; Bredt, D. S.; Snyder, S. H. Localization of phosphatidylinositol
432 signaling components in rat taste cells: role in bitter taste transduction. *Proceedings of the National*
433 *Academy of Sciences* **1990**, *87* (19), 7395-7399. DOI: 10.1073/pnas.87.19.7395.
434 15. Kinnamon, S. C.; Cummings, T. A. Chemosensory Transduction Mechanisms in Taste. *Annual*
435 *Review of Physiology* **1992**, *54* (1), 715-731. DOI: 10.1146/annurev.ph.54.030192.003435.
436 16. McLaughlin, S. K.; McKinnon, P. J.; Margolskee, R. F. Gustducin is a taste-cell-specific G
437 protein closely related to the transducins. *Nature* **1992**, *357* (6379), 563-569. DOI:
438 10.1038/357563a0.
439 17. Margolskee, R. F. The biochemistry and molecular biology of taste transduction. *Current*
440 *Opinion in Neurobiology* **1993**, *3* (4), 526-531. DOI: 10.1016/0959-4388(93)90051-y.
441 18. Pérez, C. A.; Margolskee, R. F.; Kinnamon, S. C.; Ogura, T. Making sense with TRP channels:
442 store-operated calcium entry and the ion channel Trpm5 in taste receptor cells. *Cell Calcium* **2003**,
443 *33* (5-6), 541-549. DOI: 10.1016/s0143-4160(03)00059-9.
444 19. Roper, S. D. Signal transduction and information processing in mammalian taste buds. *Pflügers*
445 *Archiv - European Journal of Physiology* **2007**, *454* (5), 759-776. DOI: 10.1007/s00424-007-
446 0247-x.
447 20. Jaggupilli, A.; Howard, R.; Upadhyaya, J. D.; Bhullar, R. P.; Chelikani, P. Bitter taste
448 receptors: Novel insights into the biochemistry and pharmacology. *The International Journal of*
449 *Biochemistry & Cell Biology* **2016**, *77*, 184-196. DOI: 10.1016/j.biocel.2016.03.005.
450 21. Carey, R. M.; Lee, R. J. Taste Receptors in Upper Airway Innate Immunity. *Nutrients* **2019**,
451 *11* (9), 2017. DOI: 10.3390/nu11092017.
452 22. Kim, K.-S.; Egan, J. M.; Jang, H.-J. Denatonium induces secretion of glucagon-like peptide-1
453 through activation of bitter taste receptor pathways. *Diabetologia* **2014**, *57* (10), 2117-2125. DOI:
454 10.1007/s00125-014-3326-5.
455 23. Deshpande, D. A.; Wang, W. C. H.; McIlmoyle, E. L.; Robinett, K. S.; Schillinger, R. M.; An,
456 S. S.; Sham, J. S. K.; Liggett, S. B. Bitter taste receptors on airway smooth muscle bronchodilate

457 by localized calcium signaling and reverse obstruction. *Nature Medicine* **2010**, *16* (11), 1299-
458 1304. DOI: 10.1038/nm.2237.
459 24. Lu, P.; Zhang, C.-H.; Lifshitz, L. M.; Zhuge, R. Extraoral bitter taste receptors in health and
460 disease. *Journal of General Physiology* **2017**, *149* (2), 181-197. DOI: 10.1085/jgp.201611637.
461 25. Carey, R. M.; McMahon, D. B.; Miller, Z. A.; Kim, T.; Rajasekaran, K.; Gopallawa, I.;
462 Newman, J. G.; Basu, D.; Nead, K. T.; White, E. A.; et al. T2R bitter taste receptors regulate
463 apoptosis and may be associated with survival in head and neck squamous cell carcinoma.
464 *Molecular Oncology* **2022**, *16* (7), 1474-1492. DOI: 10.1002/1878-0261.13131.
465 26. Miller, Z. A.; Mueller, A.; Kim, T.; Jolivert, J. F.; Ma, R. Z.; Muthuswami, S.; Park, A.;
466 McMahon, D. B.; Nead, K. T.; Carey, R. M.; et al. Lidocaine induces apoptosis in head and neck
467 squamous cell carcinoma through activation of bitter taste receptor T2R14. *Cell Reports* **2023**, *42*
468 (12), 113437. DOI: 10.1016/j.celrep.2023.113437.
469 27. Carey, R. M.; Kim, T.; Cohen, N. A.; Lee, R. J.; Nead, K. T. Impact of sweet, umami, and
470 bitter taste receptor (TAS1R and TAS2R) genomic and expression alterations in solid tumors on
471 survival. *Scientific Reports* **2022**, *12* (1). DOI: 10.1038/s41598-022-12788-z.
472 28. Royds, J.; Khan, A. H.; Buggy, D. J. An Update on Existing Ongoing Prospective Trials
473 Evaluating the Effect of Anesthetic and Analgesic Techniques During Primary Cancer Surgery on
474 Cancer Recurrence or Metastasis. *Int Anesthesiol Clin* **2016**, *54* (4), e76-83. DOI:
475 10.1097/aia.0000000000000123 From NLM.
476 29. Sessler, D. I.; Pei, L.; Huang, Y.; Fleischmann, E.; Marhofer, P.; Kurz, A.; Mayers, D. B.;
477 Meyer-Treschan, T. A.; Grady, M.; Tan, E. Y.; et al. Recurrence of breast cancer after regional or
478 general anaesthesia: a randomised controlled trial. *Lancet* **2019**, *394* (10211), 1807-1815. DOI:
479 10.1016/s0140-6736(19)32313-x From NLM.
480 30. Cakmakkaya, O. S.; Kolodzie, K.; Apfel, C. C.; Pace, N. L. Anaesthetic techniques for risk of
481 malignant tumour recurrence. *Cochrane Database Syst Rev* **2014**, (11), Cd008877. DOI:
482 10.1002/14651858.CD008877.pub2 From NLM.
483 31. Badwe, R. A.; Parmar, V.; Nair, N.; Joshi, S.; Hawaldar, R.; Pawar, S.; Kadayaprath, G.;
484 Borthakur, B. B.; Rao Thammineedi, S.; Pandya, S.; et al. Effect of Peritumoral Infiltration of
485 Local Anesthetic Before Surgery on Survival in Early Breast Cancer. *J Clin Oncol* **2023**, *41* (18),
486 3318-3328. DOI: 10.1200/jco.22.01966 From NLM.

487 32. Intratumoral Lidocaine Injection Before Oropharyngeal Cancer Surgery (856397). Clinical
488 Trials. https://clinicaltrials.gov/study/NCT06747390 (accessed.
489 33. Levit, A.; Nowak, S.; Peters, M.; Wiener, A.; Meyerhof, W.; Behrens, M.; Niv, M. Y. The
490 bitter pill: clinical drugs that activate the human bitter taste receptor TAS2R14. *The FASEB*
491 *Journal* **2014**, *28* (3), 1181-1197. DOI: 10.1096/fj.13-242594.
492 34. Margulis, E.; Slavutsky, Y.; Lang, T.; Behrens, M.; Benjamini, Y.; Niv, M. Y. BitterMatch:
493 recommendation systems for matching molecules with bitter taste receptors. *Journal of*
494 *Cheminformatics* **2022**, *14* (1). DOI: 10.1186/s13321-022-00612-9.
495 35. Wang, C.; Zhou, J.; Liu, X.; Zhu, F.; Li, J.; Xu, W.; Liu, J. Quercetin Enhances GLP-1
496 Secretion via TAS2R38-Mediated PLC Signaling in Enteroendocrine L-Cells. *Molecular Nutrition*
497 *& Food Research* **2025**. DOI: 10.1002/mnfr.70109.
498 36. Duarte, A. C.; Santos, J.; Costa, A. R.; Ferreira, C. L.; Tomás, J.; Quintela, T.; Ishikawa, H.;
499 Schwerk, C.; Schroten, H.; Ferrer, I.; et al. Bitter taste receptors profiling in the human blood-
500 cerebrospinal fluid-barrier. *Biochemical Pharmacology* **2020**, *177*, 113954. DOI:
501 10.1016/j.bcp.2020.113954.
502 37. Brenner, J. C.; Graham, M. P.; Kumar, B.; Saunders, L. M.; Kupfer, R.; Lyons, R. H.; Bradford,
503 C. R.; Carey, T. E. Genotyping of 73 UM-SCC head and neck squamous cell carcinoma cell lines.
504 *Head & Neck* **2010**, *32* (4), 417-426. DOI: 10.1002/hed.21198.
505 38. Zhao, M.; Sano, D.; Pickering, C. R.; Jasser, S. A.; Henderson, Y. C.; Clayman, G. L.; Sturgis,
506 E. M.; Ow, T. J.; Lotan, R.; Carey, T. E.; et al. Assembly and Initial Characterization of a Panel
507 of 85 Genomically Validated Cell Lines from Diverse Head and Neck Tumor Sites. *Clinical*
508 *Cancer Research* **2011**, *17* (23), 7248-7264. DOI: 10.1158/1078-0432.ccr-11-0690.
509 39. Rangan, S. R. S. A new human cell line (FaDu) from a hypopharyngeal carcinoma. *Cancer*
510 **1972**, *29* (1), 117-121. DOI: 10.1002/1097-0142(197201)29:1<117::aid-
511 cncr2820290119>3.0.co;2-r.
512 40. Fierro, F.; Peri, L.; Hübner, H.; Tabor-Schkade, A.; Waterloo, L.; Löber, S.; Pfeiffer, T.;
513 Weikert, D.; Dingjan, T.; Margulis, E.; et al. Inhibiting a promiscuous GPCR: iterative discovery
514 of bitter taste receptor ligands. *Cellular and Molecular Life Sciences* **2023**, *80* (4). DOI:
515 10.1007/s00018-023-04765-0.
516 41. Taniguchi, M.; Nagai, K.; Arao, N.; Kawasaki, T.; Saito, T.; Moritani, Y.; Takasaki, J.;
517 Hayashi, K.; Fujita, S.; Suzuki, K.-I.; et al. YM-254890, a Novel Platelet Aggregation Inhibitor

Produced by Chromobacterium sp. QS3666. *The Journal of Antibiotics* **2003**, *56* (4), 358-363. DOI: 10.7164/antibiotics.56.358.

42. Nifli, A.-P.; Theodoropoulos, P. A.; Munier, S.; Castagnino, C.; Roussakis, E.; Katerinopoulos, H. E.; Vercauteren, J.; Castanas, E. Quercetin Exhibits a Specific Fluorescence in Cellular Milieu: A Valuable Tool for the Study of Its Intracellular Distribution. *Journal of Agricultural and Food Chemistry* **2007**, *55* (8), 2873-2878. DOI: 10.1021/jf0632637.

43. Trent, T.; Miller, J. J.; Blumer, K. J.; Bowman, G. R. The G Protein Inhibitor YM-254890 is an Allosteric Glue. *Journal of Molecular Biology* **2025**, 169084. DOI: 10.1016/j.jmb.2025.169084.

44. Kim, Y.; Gumpper, R. H.; Liu, Y.; Kocak, D. D.; Xiong, Y.; Cao, C.; Deng, Z.; Krumm, B. E.; Jain, M. K.; Zhang, S.; et al. Bitter taste receptor activation by cholesterol and an intracellular tastant. *Nature* **2024**, *628* (8008), 664-671. DOI: 10.1038/s41586-024-07253-y.

45. Hu, X.; Ao, W.; Gao, M.; Wu, L.; Pei, Y.; Liu, S.; Wu, Y.; Zhao, F.; Sun, Q.; Liu, J.; et al. Bitter taste TAS2R14 activation by intracellular tastants and cholesterol. *Nature* **2024**, *631* (8020), 459-466. DOI: 10.1038/s41586-024-07569-9.

46. Peri, L.; Matzov, D.; Huxley, D. R.; Rainish, A.; Fierro, F.; Sapir, L.; Pfeiffer, T.; Waterloo, L.; Hübner, H.; Peleg, Y.; et al. A bitter anti-inflammatory drug binds at two distinct sites of a human bitter taste GPCR. *Nature Communications* **2024**, *15* (1). DOI: 10.1038/s41467-024-54157-6.

47. Kubina, R.; Iriti, M.; Kabała-Dzik, A. Anticancer Potential of Selected Flavonols: Fisetin, Kaempferol, and Quercetin on Head and Neck Cancers. *Nutrients* **2021**, *13* (3), 845. DOI: 10.3390/nu13030845.

48. Runge, A.; Mayr, M.; Schwaiger, T.; Sprung, S.; Chetta, P.; Gottfried, T.; Dudas, J.; Greier, M. C.; Glatz, M. C.; Haybaeck, J.; et al. Patient-derived head and neck tumor slice cultures: a versatile tool to study oncolytic virus action. *Scientific Reports* **2022**, *12* (1). DOI: 10.1038/s41598-022-19555-0.

49. Ma, Y. S.; Yao, C. N.; Liu, H. C.; Yu, F. S.; Lin, J. J.; Lu, K. W.; Liao, C. L.; Chueh, F. S.; Chung, J. G. Quercetin induced apoptosis of human oral cancer SAS cells through mitochondria and endoplasmic reticulum mediated signaling pathways. *Oncology Letters* **2018**. DOI: 10.3892/ol.2018.8584.

548 50. Zhang, C.; Hao, Y.; Sun, Y.; Liu, P. Quercetin suppresses the tumorigenesis of oral squamous
549 cell carcinoma by regulating microRNA-22/WNT1/β-catenin axis. *Journal of Pharmacological*
550 *Sciences* **2019**, *140* (2), 128-136. DOI: 10.1016/j.jphs.2019.03.005.
551 51. Chen, S.-F.; Nien, S.; Wu, C.-H.; Liu, C.-L.; Chang, Y.-C.; Lin, Y.-S. Reappraisal of the
552 anticancer efficacy of quercetin in oral cancer cells. *Journal of the Chinese Medical Association*
553 **2013**, *76* (3), 146-152. DOI: 10.1016/j.jcma.2012.11.008.
554 52. Haghiac, M.; Walle, T. Quercetin Induces Necrosis and Apoptosis in SCC-9 Oral Cancer Cells.
555 *Nutrition and Cancer* **2005**, *53* (2), 220-231. DOI: 10.1207/s15327914nc5302_11.
556 53. Huang, C.-F.; Liu, S.-H.; Ho, T.-J.; Lee, K.-I.; Fang, K.-M.; Lo, W.-C.; Liu, J.-M.; Wu, C.-C.;
557 Su, C.-C. Quercetin induces tongue squamous cell carcinoma cell apoptosis via the JNK
558 activation-regulated ERK/GSK-3α/β-mediated mitochondria-dependent apoptotic signaling
559 pathway. *Oncology Letters* **2022**, *23* (3). DOI: 10.3892/ol.2022.13198.
560 54. Lee, J. H.; Lee, H.-B.; Jung, G. O.; Oh, J. T.; Park, D. E.; Chae, K. M. Effect of quercetin on
561 apoptosis of PANC-1 cells. *Journal of the Korean Surgical Society* **2013**, *85* (6), 249. DOI:
562 10.4174/jkss.2013.85.6.249.
563 55. De Oliveira, M. R.; Nabavi, S. M.; Braidy, N.; Setzer, W. N.; Ahmed, T.; Nabavi, S. F.
564 Quercetin and the mitochondria: A mechanistic view. *Biotechnology Advances* **2016**, *34* (5), 532-
565 549. DOI: 10.1016/j.biotechadv.2015.12.014.
566 56. Kampa, R. P.; Sęk, A.; Szewczyk, A.; Bednarczyk, P. Cytoprotective effects of the flavonoid
567 quercetin by activating mitochondrial BKCa channels in endothelial cells. *Biomedicine &*
568 *Pharmacotherapy* **2021**, *142*, 112039. DOI: 10.1016/j.biopha.2021.112039.
569 57. De Marchi, U.; Biasutto, L.; Garbisa, S.; Toninello, A.; Zoratti, M. Quercetin can act either as
570 an inhibitor or an inducer of the mitochondrial permeability transition pore: A demonstration of
571 the ambivalent redox character of polyphenols. *Biochimica et Biophysica Acta (BBA) -*
572 *Bioenergetics* **2009**, *1787* (12), 1425-1432. DOI: 10.1016/j.bbabio.2009.06.002.
573 58. Soares, S.; Silva, M. S.; García-Estevez, I.; Groβmann, P.; Brás, N.; Brandão, E.; Mateus, N.;
574 De Freitas, V.; Behrens, M.; Meyerhof, W. Human Bitter Taste Receptors Are Activated by
575 Different Classes of Polyphenols. *Journal of Agricultural and Food Chemistry* **2018**, *66* (33),
576 8814-8823. DOI: 10.1021/acs.jafc.8b03569.

577 59. Al-Khayri, J. M.; Sahana, G. R.; Nagella, P.; Joseph, B. V.; Alessa, F. M.; Al-Mssallem, M.
578 Q. Flavonoids as Potential Anti-Inflammatory Molecules: A Review. *Molecules* **2022**, *27* (9),
579 2901. DOI: 10.3390/molecules27092901.
580 60. Hariri, B. M.; McMahon, D. B.; Chen, B.; Freund, J. R.; Mansfield, C. J.; Doghramji, L. J.;
581 Adappa, N. D.; Palmer, J. N.; Kennedy, D. W.; Reed, D. R.; et al. Flavones modulate respiratory
582 epithelial innate immunity: Anti-inflammatory effects and activation of the T2R14 receptor.
583 *Journal of Biological Chemistry* **2017**, *292* (20), 8484-8497. DOI: 10.1074/jbc.m116.771949.